The Astrophysical Journal, 782:97 (14pp), 2014 February 20 doi:10.1088/0004-637X/782/2/97

SOWING THE SEEDS OF MASSIVE BLACK HOLES IN SMALL GALAXIES: YOUNG CLUSTERS AS THE BUILDING BLOCKS OF ULTRACOMPACT DWARF GALAXIES

Pau Amaro-Seoane[1], Symeon Konstantinidis[2], Marc Dewi Freitag[3,4], M. Coleman Miller[5], and Frederic A. Rasio[6]
[1] Max Planck Institut für Gravitationsphysik (Albert-Einstein-Institut), D-14476 Potsdam, Germany; Pau.Amaro-Seoane@aei.mpg.de
[2] Astronomisches Rechen-Institut, Zentrum für Astronomie, Universität Heidelberg, Mönchhofstraße 12-14, Heidelberg D-69120, Germany; simos@ari.uni-heidelberg.de
[3] Institute of Astronomy, Madingley Road, CB3 0HA Cambridge, UK; marc.freitag@gmail.com
[4] Gymnase de Nyon, Route de Divonne 8, CH-1260 Nyon, Switzerland
[5] Department of Astronomy and Joint Space-Science Institute, University of Maryland, College Park, MD 20742-2421, USA; miller@astro.umd.edu
[6] Department of Physics and Astronomy, and Center for Interdisciplinary Exploration and Research in Astrophysics (CIERA), Northwestern University, Evanston, IL 60208, USA; rasio@northwestern.edu
Received 2012 November 28; accepted 2013 December 27; published 2014 February 3

ABSTRACT

Interacting galaxies often have complexes of hundreds of young stellar clusters of individual masses $\sim 10^4$–$10^6\ M_\odot$ in regions that are a few hundred parsecs across. These cluster complexes interact dynamically, and their coalescence is a candidate for the origin of some ultracompact dwarf galaxies. Individual clusters with short relaxation times are candidates for the production of intermediate-mass black holes of a few hundred solar masses, via runaway stellar collisions prior to the first supernovae in a cluster. It is therefore possible that a cluster complex hosts multiple intermediate-mass black holes that may be ejected from their individual clusters due to mergers or binary processes, but bound to the complex as a whole. Here we explore the dynamical interaction between initially free-flying massive black holes and clusters in an evolving cluster complex. We find that, after hitting some clusters, it is plausible that the massive black hole will be captured in an ultracompact dwarf forming near the center of the complex. In the process, the hole typically triggers electromagnetic flares via stellar disruptions, and is also likely to be a prominent source of gravitational radiation for the advanced ground-based detectors LIGO and VIRGO. We also discuss other implications of this scenario, notably that the central black hole could be considerably larger than expected in other formation scenarios for ultracompact dwarfs.

Key words: galaxies: kinematics and dynamics – galaxies: star clusters: general – gravitational waves – quasars: supermassive black holes

Online-only material: color figures

1. INTRODUCTION

Several bound systems of young, massive clusters in colliding galaxies have been observed using the *Hubble Space Telescope* (*HST*). The best studied case is the Antennæ galaxies (NGC 4038/4039), the nearest example of two colliding disk galaxies listed in the Toomre (1977) sequence. *HST* observations reveal in this system the existence of relatively small regions (compared with the size of the galaxies) harboring hundreds or thousands of young clusters (Whitmore et al. 2010, 1999; Whitmore 2006). In particular, Whitmore et al. (2010) observed 18 areas ("knots") of sizes spanning 100–600 pc which contain hundreds of clusters. The mass function of those systems, which we will henceforth refer to as "cluster complexes" (CCs), is

$$dN/dM \propto M^{\beta}, \tag{1}$$

with $\beta = -2.10 \pm 0.20$ in the range $M \sim 10^{4-5}\ M_\odot$ (see also Zhang & Fall 1999). Bastian et al. (2006) found in the same system low-mass CCs with masses around $10^6\ M_\odot$ and diameters of some 100–200 pc. One of the best studied CCs in the Antennæ galaxy is "knot S," with a total mass of $10^8\ M_\odot$ and a total radius of ∼450 pc (Whitmore et al. 1999). Other galaxies with recently discovered CCs include NGC 7673 (Homeier et al. 2002), M82 (Konstantopoulos et al. 2009), NGC 6745 (de Grijs et al. 2003), Stephan's Quintet (Gallagher et al. 2001) and NGC 922 (Pellerin et al. 2010).

CCs are bound systems (Kroupa 1998; Fellhauer & Kroupa 2005; Bruens et al. 2011; Whitmore et al. 2010) and on relatively short timescales at least some of their member clusters will merge to form a single object. Kroupa (1998) and Fellhauer & Kroupa (2005) have postulated CCs as the breeding ground of ultracompact dwarf galaxies (UCDs). Following this idea, Bruens et al. (2011) performed *N*-body simulations of CCs with different total masses ($10^{5.5}$–$10^8\ M_\odot$) and initial Plummer radii 10–160 pc. They conclude that UCDs, extended clusters (ECs) or even large globular clusters might be the product of an agglomeration of clusters in CCs. They find in their simulations that almost all members of a CC merge in less than 1 Gyr. In some cases, this timescale can be as short as 10 Myr. By the end of their simulations a very massive cluster forms in the center of the CC, with a mass of 26%–97% the mass of the initial CC and a radius of ∼50 pc.

Theoretical and numerical studies show that at least a fraction of young star clusters could host intermediate-mass black holes (IMBHs; black holes with masses ranging between 10^2–$10^4\ M_\odot$) at their centers. A possible formation path is that in a young cluster, the most massive stars sink to the center due to mass segregation. After a high-density stellar region forms, stars start to collide and merge with each other. A number of numerical studies with rather different approaches show that, under these circumstances, at least one of the stars increases its mass rapidly in a process of runaway collisions (Portegies Zwart & McMillan 2000; Gürkan et al. 2004; Portegies Zwart et al. 2004; Freitag et al. 2006a, 2006b). Nonetheless, there are a number of open questions regarding this process. One of the main uncertainties is the role of stellar winds. In principle, at

approximately solar metallicity winds may limit the mass of this very massive star (VMS) to a few hundreds of solar masses rather than a few thousands (Belkus et al. 2007). Nevertheless, we note that this requires a substantial extrapolation of already uncertain wind loss rates to stellar masses an order of magnitude beyond what is observed. Also, the collision process might lead to lumpy bags of stellar cores in an extended envelope rather than to relaxed stars near the end of the runaway collision (M. Davies 2012, private communication). In addition, when Suzuki et al. (2007) combined direct *N*-body simulations with smooth particle hydrodynamics they found that stellar winds would not hinder the formation of the VMS. It is thus possible but not certain that IMBHs can form in young clusters. We will assume their existence as a working hypothesis.

Apart from the obvious interesting implications for models of galaxy formation and, in particular, of UCDs, mergers of clusters in CCs are a powerful source of gravitational waves if these harbor central IMBHs in their respective centers (Amaro-Seoane & Freitag 2006; Amaro-Seoane et al. 2010, 2009; Amaro-Seoane & Santamaría 2010). In particular, Amaro-Seoane & Freitag (2006) showed that such mergers would lead to the formation of an IMBH binary, which would merge in a time scale as short as ∼7 Myr. Such a merger would be easily detected with space-borne observatories and also with ground-based detectors such as Advanced LIGO or Advanced VIRGO (AdLIGO/AdVIRGO) if it occurs within ∼2 Gpc (Fregeau et al. 2006). Using more realistic waveforms including spins, Amaro-Seoane & Santamaría (2010) find that the detection distance is increased significantly, up to an orientation-averaged distance of ∼5–12 Gpc, depending on the spin configuration and mass ratios. In the case of the Einstein Telescope (ET), the same authors find that the maximum redshifts for ET are $z \sim 10$, which implies that binaries of IMBHs will be a cosmological probe.

Numerical relativity simulations show that during the merger of the holes, gravitational radiation is emitted asymmetrically with the size of asymmetry depending on the mass ratio of the two black holes and on their spin magnitude and orientation (Zlochower et al. 2010; Gonzalez et al. 2007; Lousto & Zlochower 2008, 2011b; Baker et al. 2008; Lousto et al. 2010; Campanelli et al. 2007a, 2007b; Healy et al. 2009; Pretorius 2005; Sopuerta et al. 2006; Herrmann et al. 2007a, 2007b; Boyle & Kesden 2008; van Meter et al. 2010). If this recoiling velocity exceeds a few times the velocity dispersion of the merged cluster, then the IMBH leaves the host cluster. There is a massive black hole at large in the CC. Even if an IMBH escapes from one cluster, it might still be bound to the CC as a whole, which means that it has the possibility of interacting with other clusters and, perhaps, their IMBHs.

In this article, we address the formation of UCDs by the agglomeration of young clusters in CCs, along with the role of one or more recoiling IMBHs, using direct-summation *N*-body simulations. For this, we run a set of ∼200 individual experiments in which we vary mass ratios, relative speeds, and impact parameter to study in detail the interaction between a single IMBH and a cluster. We then study the interaction of one or more IMBHs at large in a CC with individual clusters with an additional set of *N*-body simulations. We correct for the trajectory of the IMBH, based on point dynamics and the mass loss in the individual clusters, by using the previous 200 experiments. We also follow the growth of a seed UCD in a CC and record all stellar disruptions triggered by the presence of the IMBH(s). For realistic models of CCs we find that the IMBH(s) end up captured by the seed UCD or by a smaller cluster which is close to the UCD. Thus, if the fraction of IMBHs in the CC ($f_\bullet$ from now onward) is not zero, this is a process of allocating one or more IMBH at the very center of a UCD.

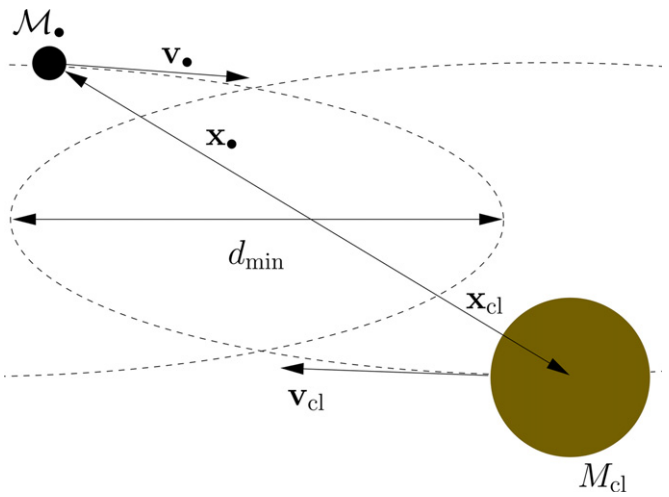

Figure 1. Geometry for the initial conditions of the parabolic collision, in the COM of the IMBH–cluster system. To obtain the grid displayed in Figure 2, we systematically vary $d_{\rm min}$, the relative velocity and the mass ratio between the IMBH and the cluster.

(A color version of this figure is available in the online journal.)

2. INTERACTIONS BETWEEN A RECOILING IMBH AND AN INDIVIDUAL YOUNG CLUSTER

In this section, we make a study of the parameter space for a collision between a recoiling IMBH and an individual young cluster in a CC. We run a set of ∼200 direct *N*-body simulations to build a grid which we will later use in our simulations of the IMBH in the CC, as explained in the introduction. Initially, we set the IMBH and the cluster on an orbit with positive relative speed and thus positive total energy in the initial state, i.e., a hyperbolic orbit, as described in Amaro-Seoane (2006). We schematically show this for reference in Figure 1 and follow a similar notation. The initial trajectory of the IMBH would bring it within a minimum distance $d_{\rm min}$ of the cluster center if the cluster was replaced by a point particle. In the center-of-mass (COM) reference frame,

$$\begin{aligned} \mathbf{x}_\bullet &= \lambda_{\rm cl}\,\mathbf{d}, \\ \mathbf{x}_{\rm cl} &= -\lambda_\bullet\,\mathbf{d}, \\ \mathbf{v}_\bullet &= \lambda_{\rm cl}\,v_{\rm rel}, \\ \mathbf{v}_{\rm cl} &= -\lambda_\bullet\,\mathbf{v}_{\rm rel}, \end{aligned} \tag{2}$$

where $\mathbf{v}_{\rm rel}$ is the relative velocity of the two objects $\mathbf{d}$ is their separation vector, $\mathbf{x}_{\bullet,{\rm cl}}$ are the positions of their centers, and $\lambda_{\bullet,{\rm cl}} = m_{\bullet,{\rm cl}}/(\mathcal{M}_\bullet + M_{\rm cl})$.

The number of stars in the cluster is always $N_\star = 3\times10^4$ and we use for their initial distribution a King model of concentration $W_0 = 7$ (King 1966; Peterson & King 1975), and all stars have the same mass, to simplify the interpretation of the results, although we note that a mass function could have an impact in the outcome of individual hits. Stellar evolution is not taken into account for the same reason. Although the number of stars we simulate is still below of what we can expect from a real cluster, we deem the dynamical interaction to be correct but for probably the most extreme mass ratios in which the mass ratio between the IMBH and the total mass in the cluster is one and two. We

include these cases for completeness but note that in those cases the stars in those clusters do not represent a single star but a set of them. That is, the IMBH will hit lighter clusters with those mass ratios, and the orbital evolution of the IMBH will be correctly estimated in our simulations, but the trajectory of a single star in such clusters does not trace one single star, but a set of them. The simulations are performed with the direct-summation NBODY4 program of Aarseth (2003). This choice was made for the sake of the accuracy of the study of the orbital parameter evolution of the IMBH and mass loss in the cluster; this numerical tool includes both the KS regularization (Kustaanheimo & Stiefel 1965) and chain regularization, which means that when two or more particles are tightly bound to each other or the separation is very small during a hyperbolic encounter, the system becomes a candidate to be regularized in order to avoid problematical small individual time steps. The basis of direct N-body codes relies on a Hermite integrator scheme (Aarseth 1999, 2003) for which we need not only the accelerations but also their time derivatives. This extra computational overhead is necessary for us to follow reliably the orbital evolution of *every* single star (or IMBH) in our system. While the code was not meant to integrate clusters in which a particle is significantly much more massive than the rest of them, a mass ratio of the order of what we have considered in this study leads to an accurate integration, with individual time integration errors of the order of 10^{-10} in energy.

At the end of an N-body run, we need to identify the particles that are still forming a bound cluster, the particles that are bound to the IMBH, and the particles that have become unbound. We also need to know whether the IMBH has been captured by the stellar cluster. We have therefore developed an iterative algorithm. To initialize the procedure, we make a (computationally) quick guess of which particles are bound to the cluster and which ones form a bound group including the IMBH (the "IMBH group"). Note that a given particle can be in both groups, for instance if the IMBH has been captured by the cluster and has sunk to its center or is orbiting it. For this first guess, stellar particles are considered bound to the IMBH group if they are bound to the IMBH (i.e., we do not take into account the self-gravity of the bound stars themselves).

For the first-guess cluster, one assumes that its center corresponds to the median position of all stellar particles, i.e., the x, y and z components of the "center" are taken to be the medians of the corresponding components of the positions of all the stellar particles. The median turns out to be a much more robust estimate of where the bulk of the particles is, compared to the average position or the COM (i.e., the mass-weighted average position) as those quantities are very sensitive to the positions of a few particles ejected at large distances from the rest. For this first guess, the 90% of the particles closest to this median position are assumed to be part of the cluster.

For the first iteration, we have to compute the binding energy of a particle relative to the cluster group, hence we need to know the velocity of that group. To estimate the velocity of the cluster in the first-guess attribution, we take the average velocity of the 10% of the particles closest to the assumed center. This number is sufficient to avoid large fluctuations due to individual particle velocities ("random velocities"). On the other hand, taking a significantly larger fraction of particles is neither necessary nor advisable as it is not yet known which particles are actually bound together as a cluster. We have to make sure that the velocity defined in the procedure is a good estimate of that of the actual bound cluster. Otherwise, the kinetic energies relative to this first-guess cluster are biased toward high values and the iterative procedure fails at identifying a bound cluster. The iterations proceed as follows. For each particle, the binding energies relative to the cluster and the IMBH group are computed. For this, we have to estimate the position of the center of each group and its velocity. For the IMBH group, they are fixed to the values of the IMBH itself. For the cluster, the center position and velocity are defined to be the mass-weighted mean values for all particles within half a "typical size" of the previous estimate of the center. The typical size of the cluster is the harmonic mean of the distance to its center (for all particles considered bound to it):

$$R_{\rm typ} = R_{\rm harm} \equiv M_{\rm cl} \left(\sum \frac{m_i}{R_i} \right)^{-1}. \quad (3)$$

One advantage of defining $R_{\rm typ}$ using the harmonic mean, instead of using the half-mass radius or some other Lagrangian radius, is that this does not require a sorting of the particles. The gravitational energy is computed assuming a spherical mass distribution, i.e., as if each particle bound to a group (cluster or IMBH group) was a spherical shell of matter, of radius R_i centered on either the IMBH position or the estimated center of the cluster. Typically, the attributions of the particles to either or both groups converge after fewer than 10 iterations.

At the end, the attributions are cleaned up in the following way. If a stellar particle belongs to both the cluster and the IMBH group, the binding energies to both structures are compared. It will be kept as member of the IMBH group only if the binding energy to the IMBH group is larger than to the cluster group. In that case, it will also be kept as member of the cluster only if the IMBH itself is bound to the cluster. This reduces the number of double-members in a reasonable way, still allowing for situations such as the IMBH having captured some stars while being itself on a bound orbit around the (main) cluster.

Finally, to interpret the results, we allow for three different outcomes. A *merger* is when the IMBH group is bound to the cluster (as determined assuming each group is a point mass) and the distance between the centers of the groups is smaller than the sum of the $R_{\rm typ}$'s. A *satellite* situation arises when the two groups are bound but the distance between their center is larger than twice the sum of the $R_{\rm typ}$'s. A *flyby* is when the groups are unbound and the distance between their centers is larger than either the sum of the total extent of each group or five times the sum of the $R_{\rm typ}$'s. Any other situation would be considered as *unknown* but does not occur if the N-body simulation has been carried out for a sufficient duration. The outcome of the simulations is depicted in Figure 2

In Figures 3 and 4 we show two particular cases for the IMBH—cluster interaction in the COM frame which, although not representative for the whole sample displayed in Figure 2, are interesting in terms of the dynamics of the system.[7] In the first case $d_{\rm min} = 1$, which leads to an almost head-on collision between the IMBH and the cluster. Nonetheless, because of the low relative velocity and mass ratio, the interaction does not lead to a huge mass loss from the cluster. Even if at $T = 45.60$ Myr the IMBH and cluster seen to be unbound, the IMBH is still

[7] The interested reader can visit http://members.aei.mpg.de/amaro-seoane/ultra-compact-dwarf-galaxies for movies based on the results of the figures (the last URL is a three-dimensional version of the second movie). The encoding of the movies is the free OGG Theora format and should stream automatically with a Gecko-based browser (such as Mozilla or Firefox) or with chromium or opera. Otherwise please see, e.g., http://en.wikipedia.org/wiki/Wikipedia:Media_help_(Ogg) for an explanation on how to play the movies.

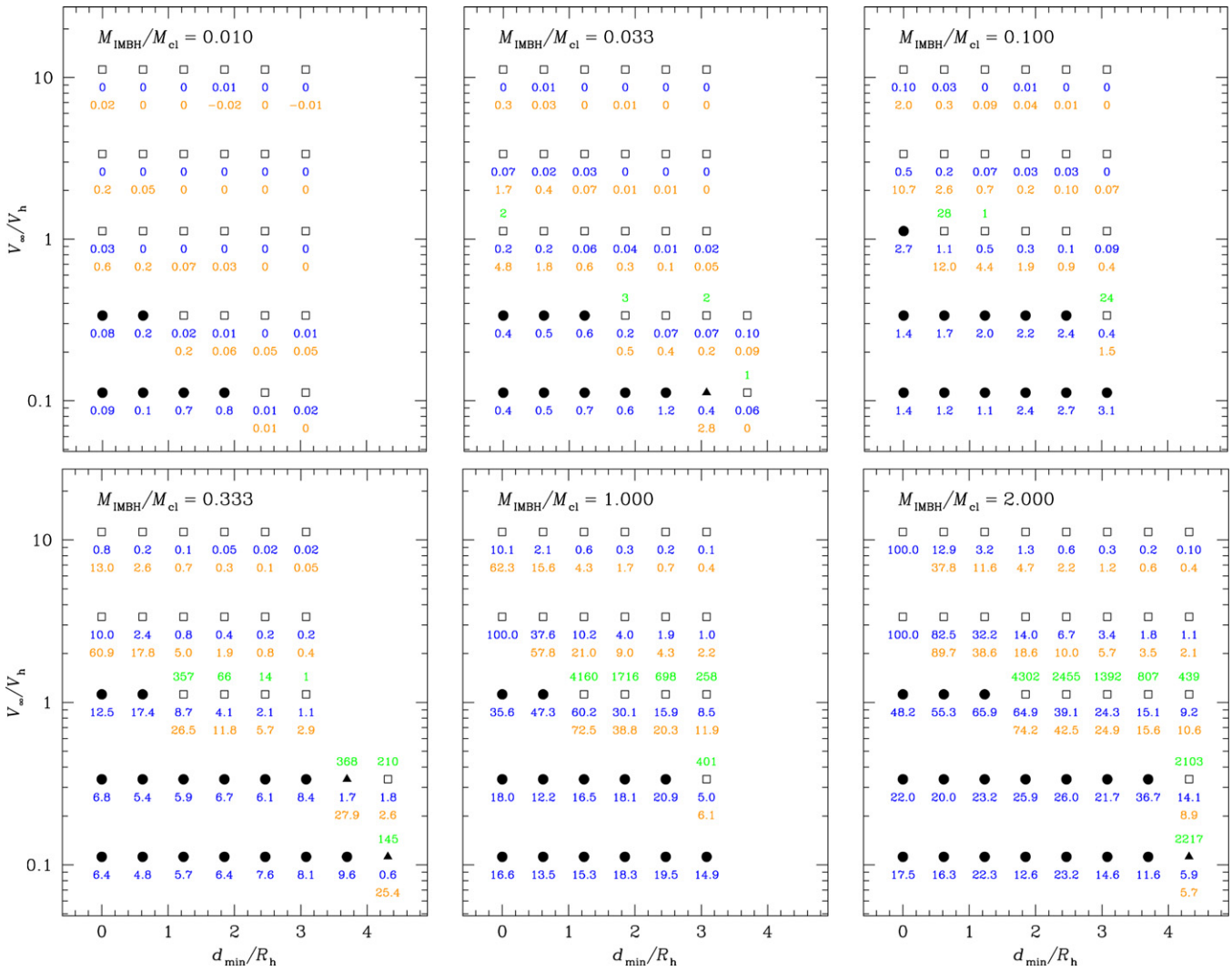

Figure 2. Outcomes of all 196 simulations of encounters between a cluster with King parameter $W_0 = 7$ and an IMBH. Each panel shows the results for a given mass ratio $\mathcal{M}_\bullet/\mathcal{M}_{\rm cl}$. The abscissa of each plot is the minimum distance $d_{\rm min}$, computed assuming two-body dynamics, in units of the half-mass radius $R_{\rm h}$. The ordinate is the relative velocity at infinity V_∞, in units of $V_{\rm h} \equiv (G\mathcal{M}_{\rm cl}/R_{\rm h})^{1/2}$, a typical velocity dispersion for the cluster. Solid round dots show "mergers," i.e., cases where the IMBH has been captured by the cluster and has settled at its center. Solid triangles are cases in which the IMBH is orbiting the cluster (a merger is likely to be the long-term outcome). Open squares are "fly-throughs." The number just below a symbol (blue) is fractional mass loss from the cluster in percent. The second, lower number (orange) is the fractional reduction in specific binding energy of the cluster, also in percent. A number above a symbol indicates how many stellar particles are bound to the IMBH (when it has not merged with the cluster).

(A color version of this figure is available in the online journal.)

forming a binary with the COM of the cluster and, hence, the semi-major axis decays again. After some 154 Myr the IMBH settles down to the center and is captured. In the second figure, the larger mass ratio has a significant impact in terms of mass loss. Already after 11.62 Myr the IMBH has captured some stars from the cluster, which remain bound to the trajectory of the hole and follow its trajectory. This satellite and the IMBH are nevertheless still gravitationally bound to the cluster and hence fall back again. The higher mass in the IMBH–satellite system leads to a rather large mass loss from the original cluster. After 80.50 Myr the IMBH is at the center of the remaining cluster.

3. INTERACTIONS BETWEEN A SINGLE RECOILING IMBH AND CLUSTERS IN A CC

3.1. Integrator and First Considerations

Now that we have completed the grid of individual IMBH-cluster interactions, we can explore the scenario in which one IMBH is at large in a CC, interacting with many different IMBH on its way, either to an eventual escape from the CC, or down to the very center, where the seed of a UCD is forming by the mergers of clusters. In this section, we will assume $f_\bullet = 2/N_{\rm tot}$, where $N_{\rm tot}$ is the total number of clusters in the CC; that is, only two clusters in the whole CC harbor an IMBH and we also assume that they have coalesced and the merged hole escaped from the host cluster. As we will see, the presence of the IMBH triggers stellar disruptions in individual clusters of the CC, which could potentially represent a fingerprint of this process. In the next section we will look at larger values of $f_\bullet$.

The numerical code that we use for the simulations of the CC and the IMBH is `Myriad` (Konstantinidis & Kokkotas 2010), which uses the Hermite fourth-order predictor-corrector scheme with block time steps (Makino & Aarseth 1992) for advancing the particles in time, while the accelerations and their derivatives are computed using GRAPE-6 (Makino et al. 2003) special purpose computers. Close encounters between particles

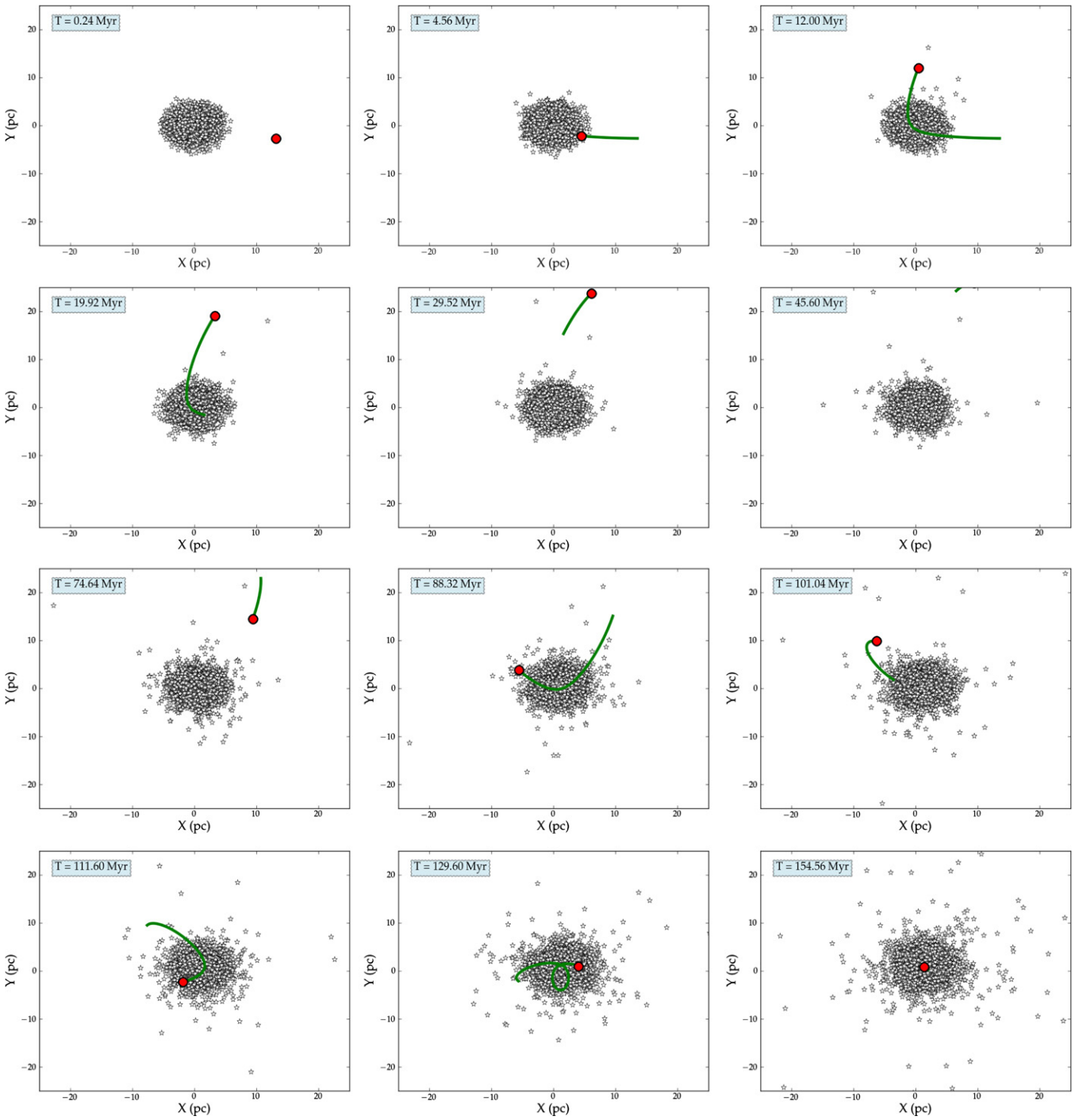

Figure 3. Projection in the X–Y plane of all trajectories of the stars (star symbols) in a cluster and the IMBH (red circle) for 12 different moments in the interaction. In this particular case, the process leads to the capture of the IMBH. For visibility, the radius of the IMBH and the stars has been artificially magnified. We also depict the previous 60 positions of the IMBH with a solid, green line. The mass ratio between the IMBH and the cluster is 0.01, the minimum distance of approach of the COM of the cluster and the IMBH is $d_{\rm min} = 1$ and $V_\infty = 1\,{\rm km\,s^{-1}}$.

(A color version of this figure is available in the online journal.)

(i.e., between clusters or between the IMBH and a cluster) are detected using the GRAPE-6 and evolved with a time-symmetric Hermite fourth-order integrator (Kokubo et al. 1998). Even though the code was originally designed for dynamical simulations of stars in star clusters, its flexible modularity made it easy to adapt to our particular problem. In particular, we assigned a radius to each particle representing a cluster, and we allowed clusters to merge with each other whenever the distance was smaller than the sum of the radii. In the simulations the IMBH is also a particle with a radius set to its Schwarzschild radius.

From the individual IMBH-cluster simulations presented previously, we have data for the outcomes based on the mass ratio $\mathcal{M}_\bullet/\mathcal{M}_{\rm cl}$, the distance of closest approach between IMBH and cluster, and the relative velocity of the two objects and, thus, the change in kinetic energy of the IMBH. We use these results to correct the position and velocity of the IMBH after each interaction with a cluster in the simulation of the CC. This

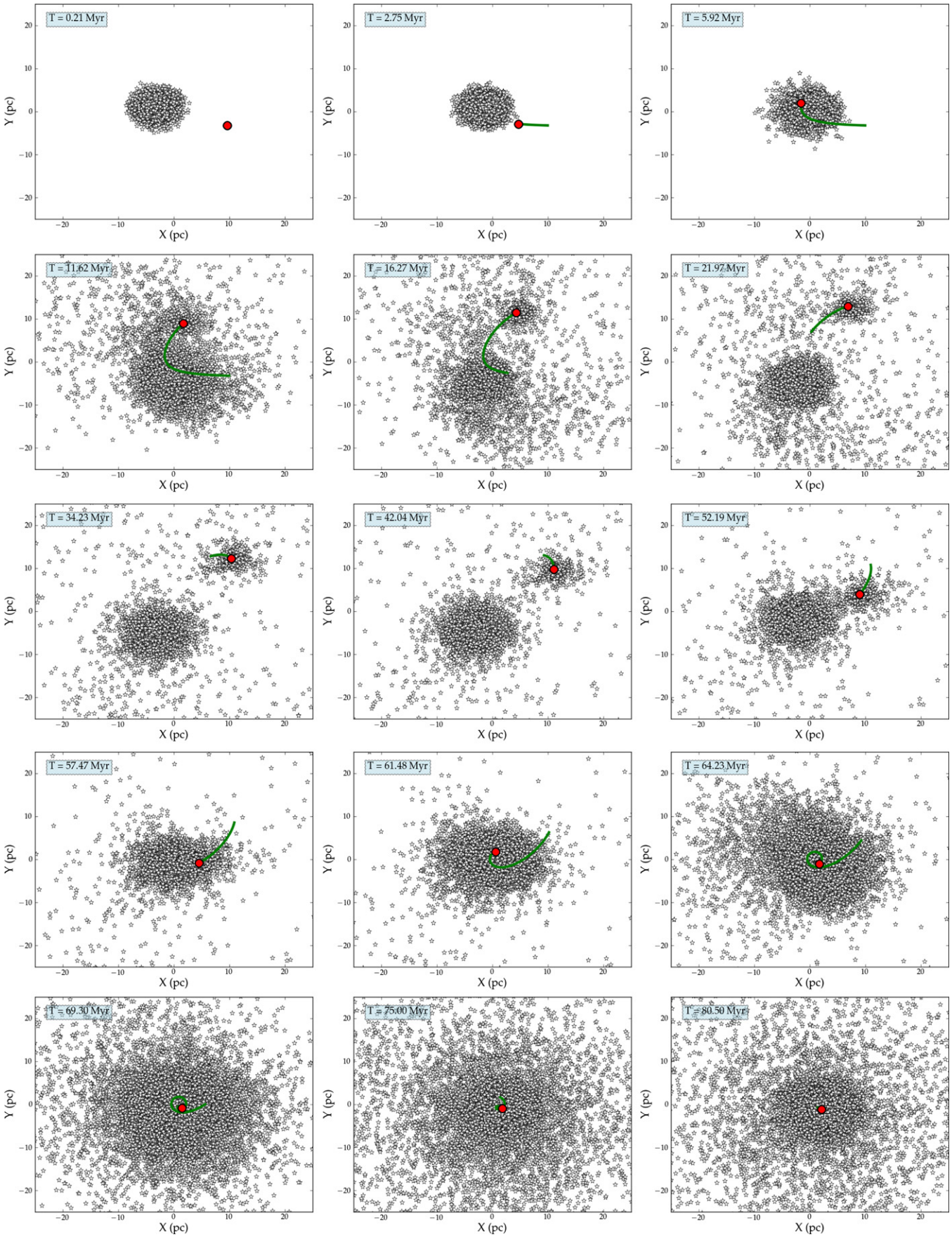

Figure 4. Same as in Figure 3 for 15 different times. The mass ratio in this case is 0.333, $d_{\rm min} = 5$ and $V_\infty = 3\,{\rm km\,s^{-1}}$.
(A color version of this figure is available in the online journal.)

also provides us with information about the number of stellar disruptions triggered by the IMBH, as well as the characteristics of the cluster which captures the IMBH (if any). If a capture does occur, the simulation finishes and then we record the position of the "trapping" cluster in the CC. Another possible termination of the simulation is if the IMBH leaves the CC, because its speed is high enough to escape the complex.

3.2. Assumptions for the Initial Conditions of the CC and the IMBH

Initially we fix the radius of the CC, $R_{\rm CC}$, to a typical value coming from observational data and populate it with individual clusters following Equation (1). In particular, in the "knots" of the Antennæ galaxy one observes a mass distribution with $n = -2$. The number of *observed* individual clusters in CCs is of the order of 100, but the actual number might actually be thousands, most of which are simply too faint to be observed (as discussed in, e.g., Fellhauer & Kroupa 2005). We set the total mass of the CC to a typical observed value, $M_{\rm CC} \sim 10^6$–$10^8\,M_\odot$. The individual clusters have half-mass radii ranging between 0.5 and 4 pc and are distributed initially in the CC following a Plummer model (Plummer 1911) with a cut off radius (see Table 1). The masses of the clusters are discrete and come from the $\mathcal{M}_\bullet/\mathcal{M}_{\rm cl}$ ratios that were used in the IMBH–cluster N-body simulations. Then, for $\mathcal{M}_\bullet = 5\times10^3\,M_\odot$ and $\mathcal{M}_\bullet/\mathcal{M}_{\rm cl} = 0.01, 0.033, 0.1, 0.33, 1, 2$, the discrete masses of the clusters in the CC are $5\times10^5\,M_\odot$, $1.51515\times10^5\,M_\odot$, $5\times10^4\,M_\odot$, $1.51515\times10^4\,M_\odot$, $5\times10^3\,M_\odot$ and $2.5\times10^3\,{\rm M}_\odot$. When two clusters collide in the CC simulation, we assume a 20% mass loss, based on the simulations of the collisions of two clusters of ? Amaro-Seoane et al. (2009), so the cluster product of the merger of two individual clusters has a mass which is 80% of the sum of the masses and a new radius, equal to the radius of the more massive cluster plus the 20% of the sum of the radii of the two clusters.

The IMBH in the merged cluster is assumed to be the product of a merger of two IMBHs that were located at the centers of two merging star clusters. We assume that this happened close to the center of the CC, where most of the individual cluster-cluster collisions take place, because this is where the numerical density of clusters is highest. Hence, we initially place the IMBH at the center of the CC. We choose a mass of $\mathcal{M}_\bullet = 5\times10^3\,M_\odot$, which determines the masses of individual clusters from the grid given in the previous section. The recoil speed of the merged IMBH could in principle be up to $\sim$5000 km s^{-1} (Herrmann et al. 2007a, 2007b; Boyle & Kesden 2008; Lousto & Zlochower 2011a, 2011b) for optimal mass ratios, spins, and spin orientations. The recoils of greatest interest to our present study are in the $\sim$100 km s^{-1} range, because the merged IMBH will then escape from its host cluster but be bound to the CC as a whole. It is difficult to judge how representative this will be for the mergers of actual IMBHs in CCs. Assuming the spin orientations are random, speeds in this range are characteristic of mass ratios $q \sim 0.1$ for substantial spins, or spins $a/M \sim 0.1$ for mass ratios comparable to unity (Lousto et al. 2010; van Meter et al. 2010). For our purposes, we will study the case of $v_{\rm recoil} = 100$ km s^{-1}. At this speed, the escape time from a cluster of total radius $\sim$10 pc is $\sim$0.1 Myr. Hence we simply place the IMBH initially at the center of the CC, not bound to any cluster, and assume that it recoils in a random direction.

For the evolution of the recoiling IMBH we must take into account the loss of kinetic energy every time it hits a cluster. In Figure 5 we can see the distribution of the resulting kinetic energy after a hit for all fly-by simulations of Figure 2. While there is a spread in the distribution, there is a strong spike around 10% of loss for about 50% of all simulations. We have therefore adopted a slightly larger value, of 20%. This loss of energy will result into a rather negligible deacceleration of the IMBH, so that it will have more chances to escape the CC, and it will also lead to a lower number of stellar tidal disruptions. On the other hand, a bit less than 50% of all "fly-throughs" have *at least* over $\sim$5% of relative loss after one hit. This situation is more appealing from a dynamical standpoint, and therefore we will first address it. In the next sections we will assume an average loss of 20% for the "fly-throughs" hits, and in Section 5 we will briefly explore the other situation.

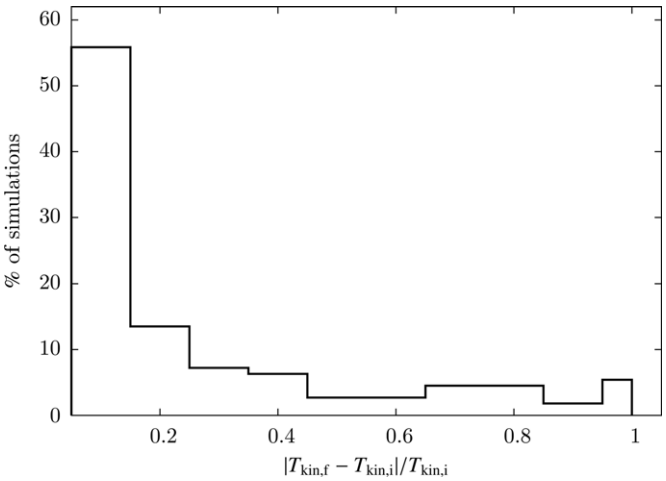

Figure 5. Kinetic energy difference between the initial and final kinetic energy ($T_{\rm kinf,\,i}$ and $T_{\rm kinf,\,f}$ respectively) normalized to the initial energy for all collisions between the IMBH and the clusters resulting in a fly-through for all N-body simulations.

Our parameter space consists of the number of clusters N and the initial radius of the CC, $R_{\rm CC}$. The total mass $M_{\rm CC}$ of the CC is a consequence of N, because the masses of the clusters are assumed to follow a power law. The total radius that we use varies from 45 pc to 330 pc. Given the mass and the size of the CCs, the initial escape speeds at the centers of the CCs are between 27 and 137 km s^{-1}. All details for all simulations are given in Table 1.

3.3. Results of the Simulations

In Figure 8 we present the results of our 34 CC simulations. In simulations A1–A5, B1–B5, C1–C4, D1–D4, E3–E4, F4, G4, and H4 the IMBH escapes the CC after between zero and a few interactions with clusters. These cases correspond to smaller-mass CCs or to low initial concentrations. In simulations E1–E2, F1–F3, G1–G3, and H1–H4, which are more representative of observed CCs, the IMBH is captured in the CC after a significant number of interactions and ends up being trapped by an individual cluster, which can be the UCD seed (cases E1, E2, F2, F3, and H2). We show two particular cases which led to the capture of the IMBH in Figures 6 and 7.

The IMBH goes through a very large number of interactions with individual clusters until it is eventually trapped. This number depends on the density of clusters in the CC. In six simulations, the IMBH gets captured by a cluster that has not yet merged with other clusters. In five simulations, the cluster that captures the IMBH is the central cluster of the CC, the seed UCD. We show in Table 2 the details about the cluster that captures the IMBH, the distance from the center where this takes

Table 1
Simulation ID, Number of Clusters, Total Mass, and Cut-off Radius of the CC

ID	N	$M_{\rm CC}$ ($M_\odot$)	$R_{\rm CC}$ (pc)	ID	N	$M_{\rm CC}$ ($M_\odot$)	$R_{\rm CC}$ (pc)
A1	5×10^2	1.522×10^7	45	E1	3×10^3	4.32×10^7	122
A2	5×10^2	1.522×10^7	90	E2	4×10^3	5.75×10^7	165
A3	5×10^2	1.522×10^7	132	E3	4×10^3	5.75×10^7	246
A4	5×10^2	1.522×10^7	168	E4	4×10^3	5.75×10^7	329
A5	5×10^2	1.522×10^7	255				
B1	1×10^3	1.522×10^7	90	F1	5×10^3	7.18×10^7	122
B2	1×10^3	1.522×10^7	128	F2	5×10^3	7.18×10^7	165
B3	1×10^3	1.522×10^7	169	F3	5×10^3	7.18×10^7	248
B4	1×10^3	1.522×10^7	252	F4	5×10^3	7.18×10^7	330
B5	1×10^3	1.522×10^7	333				
C1	2×10^3	2.9×10^7	126	G1	6×10^3	8.6×10^7	122
C2	2×10^3	2.9×10^7	167	G2	6×10^3	8.6×10^7	165
C3	2×10^3	2.9×10^7	252	G3	6×10^3	8.6×10^7	248
C4	2×10^3	2.9×10^7	336	G4	6×10^3	8.6×10^7	330
D1	3×10^3	4.32×10^7	124	H1	8×10^3	1.14×10^8	122
D2	3×10^3	4.32×10^7	166	H2	8×10^3	1.14×10^8	165
D3	3×10^3	4.32×10^7	249	H3	8×10^3	1.14×10^8	248
D4	3×10^3	4.32×10^7	332	H4	8×10^3	1.14×10^8	330

Note. Note that the table is vertically split in two subtables.

Table 2
Data for the Simulations Where the IMBH Was Captured by a Cluster of the CC

ID	Coll	T [Myr]	$R_{\rm capt}$ [pc]	$\mathcal{M}_{\rm cl}$ [$M_\odot$]	$\mathcal{M}_{\rm UCD}$ [$M_\odot$]	$T_{\rm DF}$ [Myr]	$T_{\rm FH}$ [Myr]	$T_{\rm FC}$ [Myr]
E1	1	14	9.6	1.9×10^6	1.9×10^6	142	0.197	12.57
E2	0	38.2	10.3	1.2×10^6	1.2×10^6	129	0.09	33.59
F1	4	9.7	42	5×10^3	6.5×10^5	2400	0.047	2.14
F2	9	28.2	18.4	7.3×10^5	7.3×10^5	240	0.067	0.54
F3	6	118	15.4	2.9×10^6	2.9×10^6	367	0.1	0.28
G1	3	10.14	45.6	2.5×10^3	1.1×10^6	4300	0.011	0.35
G2	3	13.1	23.8	1.5×10^4	6.6×10^5	762	0.009	0.009
G3	11	167.4	92.7	2.5×10^3	4×10^6	7900	0.1	44.8
H1	4	11.7	15.5	5.6×10^5	1.3×10^6	26	0.012	3.65
H2	9	20.1	17.8	1.8×10^6	1.8×10^6	360	0.15	5.32
H3	11	49.9	30.2	1.5×10^5	9.7×10^5	167	0.28	9.54

Notes. The first column shows the ID of the simulation (see Table 1). The second column shows the number of stellar collisions triggered by the IMBH. The third column displays the time of capture of the IMBH by a single cluster. The fourth shows the distance from the center of the CC, where the IMBH was captured. The next column gives us the mass of that cluster and the mass of the heaviest cluster in the CC by that time; i.e., the mass of the forming UCD. The sixth column corresponds to an estimate for the IMBH to reach the center of the CC by dynamical friction (see the text). The last two columns show the time the IMBH hits a cluster for the first time and the time of the first stellar collision in the CC. In the particular case of simulation F1 there was a tidal disruption of a star by the IMBH.

place, and the mass of the most massive cluster in the system at the time of the IMBH-capture, i.e., the mass of the UCD seed. An interesting process in the dynamical evolution of the system is that the IMBH triggers stellar collisions, i.e., stars are set on such an orbit that they collide and disappear from the system. We note that only in one case, in simulation F1, one star was torn apart by the tidal forces of the IMBH acting on a star. The middle number next to each circle of Figure 8 corresponds to star–star *collisions triggered by the IMBH* in the clusters. We can conclude that one should expect a star–star collision in a CC every 5–8 Myr. In Figure 9 we show the accumulated number of stellar collisions that led to a disruption in function of the time for simulation G3, as well as the accumulated number of hits between the IMBH and a cluster.

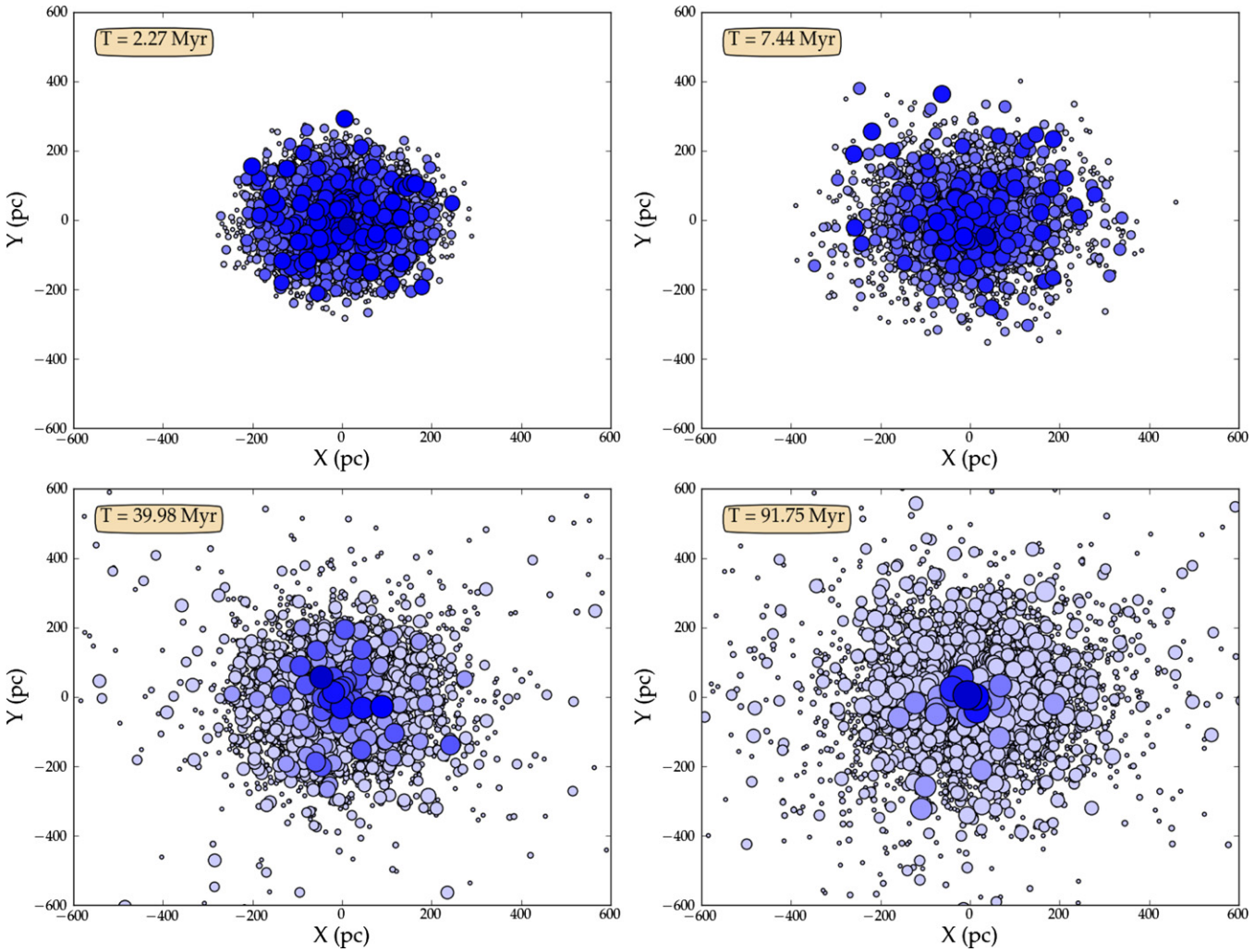

Figure 6. Formation of the UCD seed at the center of the CC. We show a projection in the X–Y plane of all individual clusters for the simulation F3. The radii of the clusters have been artificially magnified, heavier members have larger sizes and darker colors *relative to every panel for the sake of visibility*. This means that even if the colors of the heaviest clusters in the last panel are as dark as the most massive ones in the first panel, the clusters in the last panel are heavier and larger. After 7.44 Myr we can already see how the more massive clusters start to agglomerate at the center of the CC. Later, at $T \sim 40$ Myr, all of them are confined to the central part of the CC and in the last panel we can see that only a handful of clusters are heavy and a very massive cluster is sitting at the very center, while lighter clusters occupy all of the remaining space. The mass of this very massive cluster is $2.9 \times 10^6\ M_\odot$ and constitutes the seed of the UCD. See http://members.aei.mpg.de/amaro-seoane/ultra-compact-dwarf-galaxies, model F3, for an animation of the process.

(A color version of this figure is available in the online journal.)

The third number next to each circle of Figure 8 is the initial escape velocity at the center of the CC. As it is obvious, CCs with values <100 km s^{-1} retain the IMBH due to our choice of the initial recoiling speed. An interesting case is simulation H4 in which the escape velocity is 84 km s^{-1}, but the IMBH escapes because the system is initially not very concentrated and the IMBH has only two interactions with clusters. In this case, the energy of the IMBH did not decrease enough to be trapped in the CC. Simulation G3 corresponds to the opposite situation. Even though the escape speed is the same as in H4, the IMBH remains in the system because the CC is denser, so that the IMBH has a chance of interacting significantly with clusters and, hence, of decreasing its kinetic energy below the threshold. In Figure 10 we have the evolution of the velocity of the IMBH in simulation G3 compared with the escape velocity at the radius of the CC where the IMBH is. Initially, the escape velocity is lower than the velocity of the IMBH, ensuring the escape of the IMBH from the system, but the IMBH loses energy rapidly during the first few Myr because of its interactions with clusters.

4. INTERACTIONS BETWEEN MULTIPLE RECOILING IMBHs AND CLUSTERS IN A CC

In this section, we investigate a scenario in which $f_\bullet > 1$. We use the initial configuration of F3 as described in Table 1 as our fiducial CC system and study the evolution of systems of five and ten IMBHs at large. For this, we set them initially close to the center and allow them to be kicked off the host cluster at the same time, $T = 0$, as a simplifying assumption. In real systems there will be a time lag:

$$\tau_{\rm bin} = \tau_{\rm run}\, \tau_{\rm IMBH}\, \tau_{\rm merg}, \tag{4}$$

where $\tau_{\rm run}$ is the timescale for a cluster to evolve to the runaway phase, $\tau_{\rm IMBH}$ is the timescale for the VMS to become unstable and form an IMBH and $\tau_{\rm merg}$ is the timescale for the cluster to merge with another cluster. The phenomena involved are various and the assumptions inherent to $\tau_{\rm run}$ and $\tau_{\rm IMBH}$ prevent realistic estimates, as we explained in the introduction. On the other hand, Amaro-Seoane & Freitag (2006) estimate that

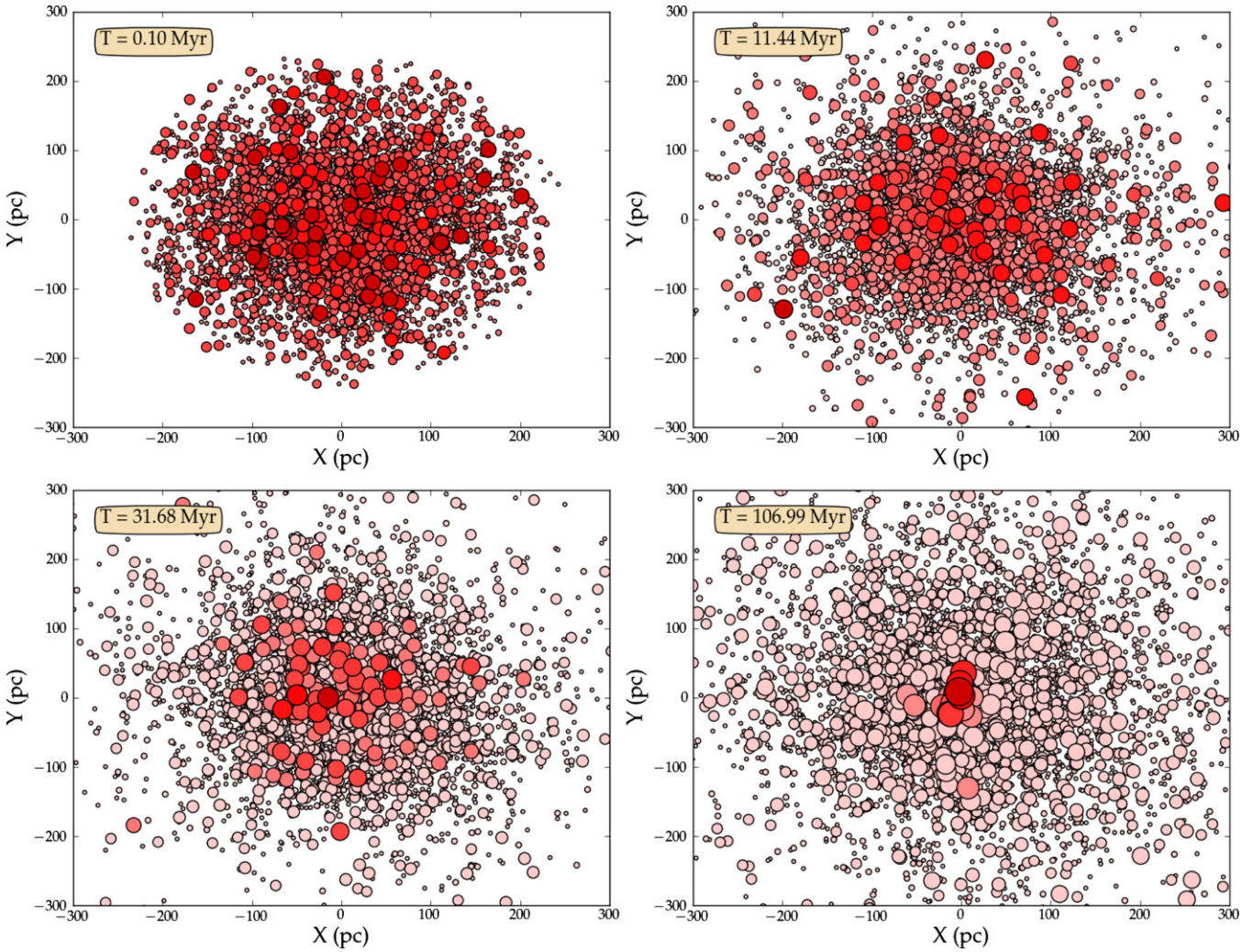

Figure 7. Same as in Figure 6 but for simulation G3. In this case we show a zoom of diameter 600 pc. As in the first figure, after some ∼100 Myr we have a very massive cluster at the center and all other clusters are much lighter. The heaviest cluster at this time has a mass of $5.5 \times 10^5\,M_\odot$, while clusters with masses $5.2 \times 10^5\,M_\odot$, $5.0 \times 10^5\,M_\odot$, $1.9 \times 10^5\,M_\odot$, $1.4 \times 10^5\,M_\odot$, and $6.5 \times 10^4\,M_\odot$ lie very close to the center of the CC. See http://members.aei.mpg.de/amaro-seoane/ultra-compact-dwarf-galaxies, model G3, for a movie of the figure.

(A color version of this figure is available in the online journal.)

$\tau_{\rm merg} \sim 7$ Myr, which compared to the timescale for the CC to reach the seed UCD phase, of the order of ∼100 Myr, is a rather short interval of time and can be regarded as instantaneous. In view of these arguments, we assume that the IMBHs are expelled instantaneously from their host clusters at different places of the CC at $T = 0$.

In Table 3 we show the results for the first simulation, in which we place five IMBHs around the center, as indicated in column number three. IMBHs 2–5 have been distributed over the surface of a sphere of radius 17.32 pc and only one, 1, is very close to the center, to avoid the artificial formation of various binaries of IMBHs when we start the simulation. We assign the holes initial recoil speeds between 50 and 100 km s^{-1} and different directions and then let the system evolve. We find that after some ∼34 Myr all IMBHs have been either captured by an individual cluster which is sinking the center due to DF, or formed a satellite with a cluster. In Figure 11 we show the CC at $T = 62.37$ Myr. We stop the simulation at that time because the satellites are consuming all of the computational power. In the process and up to that time, there are seven stars that have been disrupted in the CC, as we can see in the table.

In Table 4 we repeat the same exercise but for a system with 10 IMBHs. The initial setup is identical to the previous one. We find that in this case three holes leave the system due to an increase in their kinetic energy. The rest of them have formed a hard binary with a cluster and will eventually be captured.

5. LOWER KINETIC ENERGY LOSS

In the simulations of the previous sections we assumed a loss of relative kinetic energy of ∼20% for the hits that led to a fly-through, although it could be much larger than that, as we saw in Figure 5. While this is true for a bit less than 50% of all systems, the rest of them had a peak in the distribution around ∼5%. We have addressed the situation of a larger loss first, because it leads to more interesting effects from a pure dynamical standpoint.

However, we deem it necessary to we repeat some experiments in the evolution of the CC to understand the other regime. Therefore, we repeat experiments G1–G4, H1, H3, and H4 of Table 1 but this time we assume a loss of 5% after every hit for the fly-throughs. In Figure 12 we can see the results. We have reduced the exploration to the range of radii and total mass

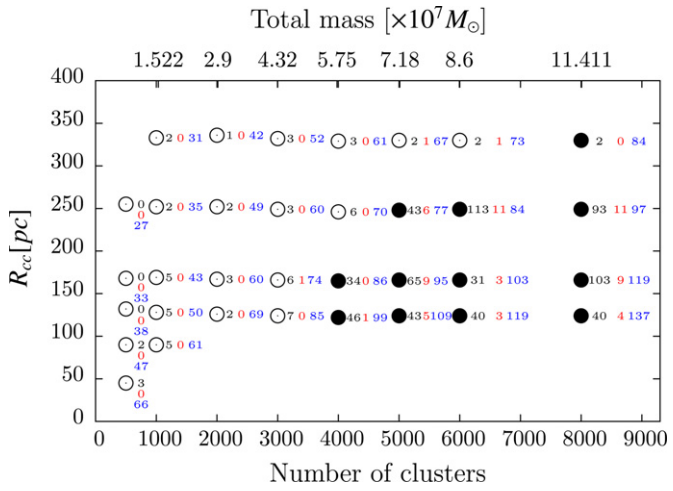

Figure 8. Outcome of the CC simulations. The *x*-axis shows the number of clusters in each simulation, while the *y*-axis shows the initial radius of the CC. The upper *x*-axis shows the total mass of the system in $M_\odot$. Every circle corresponds to a single entry of Table 1 in a way such that the circle at the bottom left corresponds to the simulation with ID A1 and the circle at the top right corresponds to the simulation with ID H4. An open circle indicates a simulation where the IMBH finally escaped the CC. On the other hand, a filled circle represents a simulation where the IMBH remained bound to the system. Next to every circle there are three numbers. The first (black) shows the number of clusters hit by the IMBH until either it escapes the CC or it is captured by a cluster. The second (red) number is the number of stars that are tidally disrupted by the IMBH and the number of star–star collisions triggered by the IMBH in the clusters. The third number indicates the initial escape velocity at the center of the CC in $\mathrm{km\,s^{-1}}$.

(A color version of this figure is available in the online journal.)

that could be more interesting for our analysis. We can see that although the total number of stellar disruptions is significantly reduced, it is not zero. Also, in four configurations the IMBH at large is captured eventually by the forming CC.

6. SUMMARY AND CONCLUSIONS

In this work we have presented results that address the formation of UCD from young clusters, and the role of recoiling IMBHs in a CC. The formation of the IMBH in clusters is used as a working hypothesis, and hence also the possibility that these interact with the young clusters. For that, we first ran a set of ∼200 direct-summation *N*-body simulations that covers the parameter space for individual IMBH–cluster encounters. We methodically varied the mass ratio between the IMBH and the cluster, the relative velocity, and the impact parameter. This allowed us to build a grid with the expected outcome of the interaction and the modification of the kinetic energy of the IMBH. Later we ran additional direct-summation *N*-body simulations for a scenario in which one IMBH is at large in a CC. The IMBH is assumed to be the result of the coalescence of two holes, which led to the expulsion of the hole from the initial host cluster. We studied the dynamical evolution of this single IMBH in an evolving CC. Parallel to the individual interactions between the IMBH and clusters in the CC, which are corrected using the above-mentioned table, clusters are colliding and merging with each other, which results in the formation of a run-away individual cluster, which typically after ∼100 Myr contains almost all of the mass of the CC. This is what we designate "the seed of an UCD," since this very massive cluster is the result of the successive amalgamation of smaller clusters in the initial distribution of the CC.

We find that for realistic CCs (i.e., those which resemble observations, such as the knots of the Antennæ), the IMBH is either eventually captured by the seed UCD (in those simulations less dense initially) or by a smaller cluster (in the simulations with the largest concentrations of clusters at the center) which, however, is close to the center of the CC, so that it will in the course of time sink down to the very center, where the seed UCD is settled. The typical timescale for this trapping is of about ∼200 Myr.

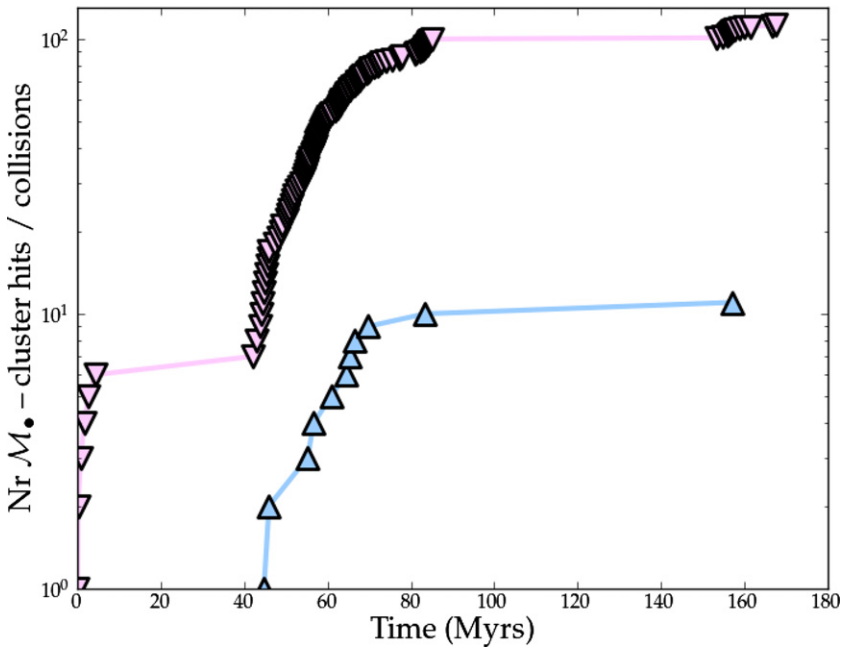

Figure 9. Cumulative number of IMBH and cluster hits for the simulation G3 (inverted, light magenta triangles) and of stellar collisions leading to a disruption (blue triangles) as a function of time.

(A color version of this figure is available in the online journal.)

Table 3
Data for the Simulation with Five IMBHs in a CC

IMBH ID	Outcome	$R_{\rm init}$ (pc)	$V_{\rm init}/V_{\rm esc}$	T (Myr)	$R_{\rm fin}^{\rm UCD}$ (pc)	$M_{\rm cl}$ ($M_\odot$)	Stellar Disr
1	Capture	0.0024	0.89	14.24	51.2	2.5×10^3	1
2	Capture	17.32	0.70	12.41	103	7.85×10^5	2
3	Satellite	17.32	0.71	34	0	9.6×10^5	2
4	Satellite	17.32	0.94	9.45	9.5	5.44×10^5	1
5	Capture	17.32	0.76	2.35	118.2	5×10^5	1

Notes. The first column shows the ID of the IMBH, the second column the outcome of the BH after 35 Myr, which can be either a capture, a satellite (the IMBH is orbiting a cluster and will eventually merge with it), or an escape (the IMBH escapes the whole CC). The third column displays the initial distance of the IMBH from the center of the CC. The fourth corresponds to the initial velocity of the normalized to the local escape velocity from the cluster. The fifth gives the time at which the outcome was measured. The sixth shows the final distance of the capturing cluster from the most massive cluster of the system, the seed UCD. In this case, IMBH 3 is captured by the seed, and thus this distance is zero. The seventh is the mass of the capturing cluster at the time of capture. Finally, the last column shows the number of stellar collisions in clusters that have been triggered by the IMBH.

Table 4
Same as in Table 3 but for 10 Holes

IMBH ID	Outcome	$R_{\rm init}$ (pc)	$V_{\rm init}/V_{\rm esc}$	T (Myr)	$R_{\rm fin}^{\rm UCD}$ (pc)	$M_{\rm cl}$ ($M_\odot$)	No. of Stellar Disr
1	Satellite	0.0018	0.56	1.9	130.7	7.5×10^5	2
2	Satellite	17.33	0.97	23.8	130.7	1.6×10^6	2
3	Satellite	17.33	0.99	8.9	112.2	1.44×10^6	3
4	Satellite	17.33	0.89	9.1	163.5	2.2×10^6	1
5	Escaper	17.33	0.56	...	...	...	5
6	Escaper	17.33	0.59	...	...	...	0
7	Escaper	17.33	0.88	...	...	...	7
8	Satellite	17.33	0.90	10.2	8.7	2.7×10^6	1
9	Satellite	17.33	0.56	5.7	140.5	7.75×10^6	0
10	Satellite	25.99	0.72	4.4	140.5	1.47×10^6	1

Notes. In this case three IMBHs leave the CC. We find 22 stellar disruptions during the simulation.

We can see this by estimating the dynamical friction time $T_{\rm DF}$. This is the timescale for the IMBH captured in a cluster to reach the center. For an object with mass m moving in a system of total mass M it is given by (see, e.g., Binney & Tremaine 2008)

$$T_{\rm DF} = \frac{1.17}{\ln \Lambda} \frac{M}{m} \frac{r}{V_h}, \quad (5)$$

where r is the distance from the center of the system, V_h is the root mean square velocity dispersion of the system and $\ln \Lambda$ the Coulomb logarithm, which is of the order of unity. From Table 2 we can see that in almost half of the cases in which the IMBH was retained in the CC, it is captured by the most massive cluster of the system, the seed UCD. $T_{\rm DF}$ is in all cases a few tens or hundreds of Myr. On the other hand, when the IMBH gets captured by a smaller cluster (6 out of the 11 simulations), $T_{\rm DF}$ is of the order of $\sim$1 Gyr, still well below a Hubble time. We note also that this analytical calculation is an overestimate, because the CC evolves dynamically with time and there is a huge accumulation of mass in the innermost region which will significantly reduce the timescale for the IMBH to reach the seed UCD.

When the IMBH remains bound to the CC, the average time for it to hit a cluster is 0.16–0.43 Myr. On the other hand, the mean time taken by the IMBH to fly through a star cluster is of the order of 0.1 Myr. Hence, after recoiling and before getting captured, the IMBH spends one-third of its time interacting with clusters, so that the possibility to find an IMBH in a cluster of a newly formed (less than 100 Myr old) CC is about $\sim$30%

We repeated the exercise with a CC harboring initially 5 and 10 IMBHs which were distributed with different velocities. We find that after some $\lesssim$30 Myr most of the holes are either captured by a single cluster or have formed a hard binary with one in regions relatively close to the runaway cluster, the seed of a UCD which is forming in the CC. We cannot follow the further evolution of the system due to the limitations inherent to our approach. We also note that gas is very likely to play an important role in the whole process. In particular, in some CCs the oldest cluster is located at the center of the gas cloud (Whitmore et al. 2010). In our simulations we have neglected this, since we are limited by our codes, which rely on pure particle dynamics. Still, even if we could actually have implemented a (rough) approach for the gas with an external force, the complexity of the problem justifies our first approach. We have decided to postpone the role of the gas for upcoming work. The same applies to mass loss because of stellar evolution, although statistically, since the IMBH interacts with clusters of different masses, the global dynamical evolution is well represented by our models, within our limitations.

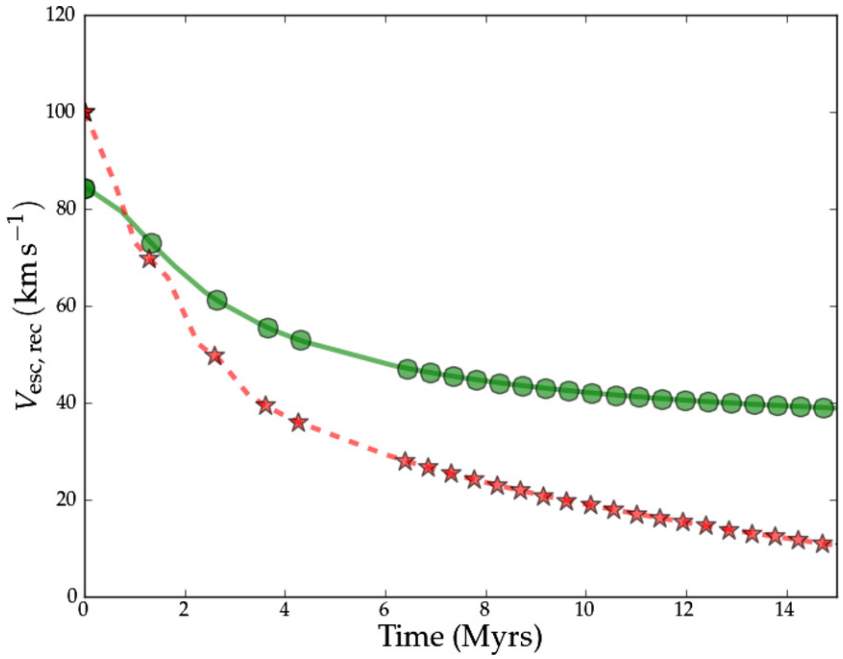

Figure 10. IMBH speed (dashed, red line with stars) and instantaneous escape velocity (solid, green curve with spheres) for the IMBH as a function of time in simulation G3. Even though initially the IMBH recoiling speed is higher than the required threshold to escape the CC, soon after ∼0.80 Myr the interactions with individual clusters lower its kinetic energy and it is trapped in the CC, in the meaning that the speed drops below the threshold.

(A color version of this figure is available in the online journal.)

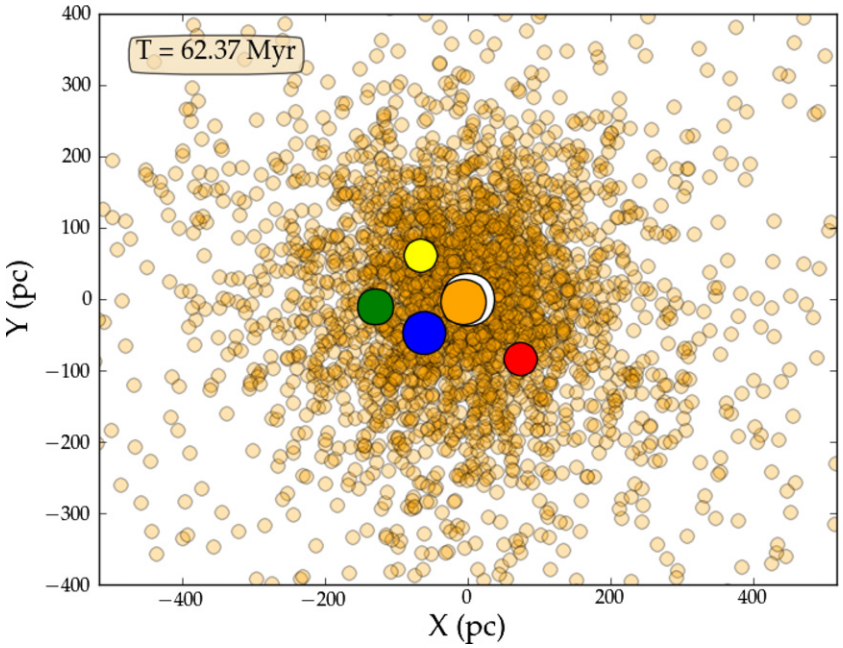

Figure 11. Projection in *X*–*Y* of all clusters for the simulation in which we have initially five IMBHs. We show in white, orange, blue, green, yellow, and red the clusters that captured the holes (or will capture, if in satellite; see the text). For clarity we depict all other clusters with the same radius and color (light orange). The green cluster harbors two IMBHs and the blue cluster too. The later one merged with an IMBH and after that with another one which contained another IMBH.

(A color version of this figure is available in the online journal.)

Also, reducing the relative kinetic energy loss for fly-throughs leads to a reduced number of tidal disruption events, but we still find some systems for which the implications are similar to the analysis that used a larger loss.

While the number fraction of IMBH in the mass-range of 10^2–10^4 $M_\odot$ in CCs is an unknown, they sink to the center in a time which is much shorter than the Hubble time. The scenario that we have described here leads to the formation of a very massive black hole at the center of the UCD, with a mass that depends on unknowns, such as the formation rate of IMBHs in the CC. The internal velocities of the systems we study are not as extreme as those explored by Merritt et al. (2009) in the context of hypercompact stellar systems, because the seed UCD inherits the central velocity from the resulting mergers between individual clusters. When the UCD is formed, the velocity will roughly be what one can expect from a dense stellar system

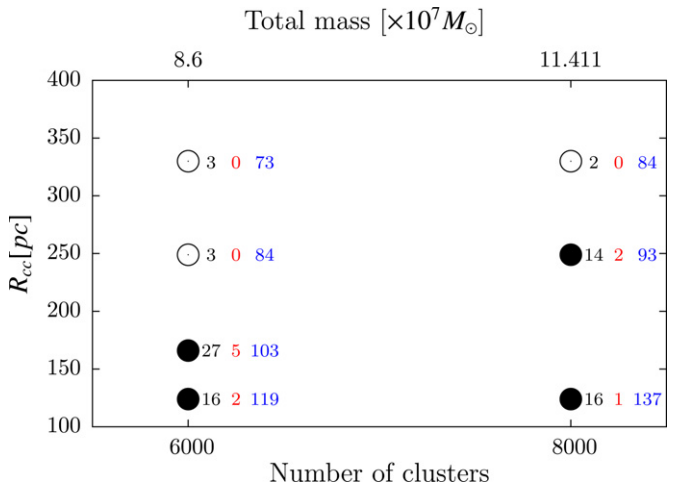

Figure 12. Same as Figure 8 but assuming a fixed loss of kinetic energy of 5% after every hit for the fly-throughs.

(A color version of this figure is available in the online journal.)

in dynamical equilibrium. A very interesting feature of the process of sowing an UCD with an IMBH is that independently of whether the IMBH stays in the CC or escapes, it triggers star–star collisional disruptions in the clusters it hits. This could be envisaged as an electromagnetic signature of the scenario.

It is a pleasure for P.A.S. to thank Rainer Schödel and Emilio Alfaro for their invitation to the IAA, where some of the work was done. He is particularly indebted to Rainer and Elena Navajas for their support and for the psetta maxima. This work was supported in part by the National Science Foundation under grant No. 1066293 and the hospitality of the Aspen Center for Physics. The work of S.K. was funded by the German Science Foundation (DFG) via SFB/TR7 on "Gravitational Waves" and the German Academic Excange Service (DAAD). M.C.M. was supported in part by NASA ATP grants NNX08AH29G and NNX12AG29G. F.A.R. acknowledges support from NSF Grant PHY-0855592 and NASA Grant NNX08AG66G. The use of the GRAPE-6 system of the University of Thessaloniki was supported by a grant by the Empirikion Foundation. We acknowledge the usage of the Tuffstein GRAPE cluster at the AEI.

REFERENCES

Aarseth, S. J. 1999, PASP, 111, 1333
Aarseth, S. J. 2003, Gravitational N-Body Simulations (Cambridge: Cambridge Univ. Press)
Amaro-Seoane, P. 2006, in AIP Conf. Proc. 873, Laser Interferometer Space Antenna: 6th International LISA Symposium, ed. S. M. Merkovitz & J. C. Livas (Melville, NY: AIP), 250
Amaro-Seoane, P., Eichhorn, C., Porter, E. K., & Spurzem, R. 2010, MNRAS, 401, 2268
Amaro-Seoane, P., & Freitag, M. 2006, ApJL, 653, L53
Amaro-Seoane, P., Miller, M. C., & Freitag, M. 2009, ApJL, 692, L50
Amaro-Seoane, P., & Santamaría, L. 2010, ApJ, 722, 1197
Baker, J. G., Boggs, W. D., Centrella, J., et al. 2008, ApJL, 682, L29
Bastian, N., Emsellem, E., Kissler-Patig, M., & Maraston, C. 2006, A&A, 445, 471
Belkus, H., Van Bever, J., & Vanbeveren, D. 2007, ApJ, 659, 1576
Binney, J., & Tremaine, S. (ed.) 2008, Galactic Dynamics (2nd ed.; Princeton, NJ: Princeton Univ. Press)
Boyle, L., & Kesden, M. 2008, PhRvD, 78, 024017
Bruens, R. C., Kroupa, P., Fellhauer, M., Metz, M., & Assmann, P. 2011, A&A, 529, 138
Campanelli, M., Lousto, C., Zlochower, Y., & David, M. 2007a, PhRvL, 98, 1102
Campanelli, M., Lousto, C. O., Zlochower, Y., & David, M. 2007b, ApJ, 659, 5
de Grijs, R., Anders, P., Bastian, N., et al. 2003, MNRAS, 343, 1285
Fellhauer, M., & Kroupa, P. 2005, MNRAS, 359, 223
Fregeau, J. M., Larson, S. L., Miller, M. C., O'Shaughnessy, R., & Rasio, F. A. 2006, ApJL, 646, L135
Freitag, M., Gürkan, M. A., & Rasio, F. A. 2006a, MNRAS, 368, 141
Freitag, M., Rasio, F. A., & Baumgardt, H. 2006b, MNRAS, 368, 121
Gallagher, S. C., Charlton, J. C., Hunsberger, S. D., Zaritsky, D., & Whitmore, B. C. 2001, AJ, 122, 163
Gonzalez, J. A., Hannam, M., Sperhake, U., Brgmann, B., & Husa, S. 2007, PhRvL, 98, 231101
Gürkan, M. A., Freitag, M., & Rasio, F. A. 2004, ApJ, 604, 632
Healy, J., Herrmann, F., Hinder, I., et al. 2009, PhRvL, 102, 041101
Herrmann, F., Hinder, I., Shoemaker, D., & Laguna, P. 2007a, CQGra, 24, 33
Herrmann, F., Hinder, I., Shoemaker, D., Laguna, P., & Matzner, R. A. 2007b, ApJ, 661, 430
Homeier, N., Gallagher, J. S. I., & Pasquali, A. 2002, A&A, 391, 857
King, I. R. 1966, AJ, 71, 276
Kokubo, E., Yoshinaga, K., & Makino, J. 1998, MNRAS, 297, 1067
Konstantinidis, S., & Kokkotas, K. D. 2010, A&A, 522, 70
Konstantopoulos, I. S., Bastian, N., Smith, L. J., et al. 2009, ApJ, 701, 1015
Kroupa, P. 1998, MNRAS, 300, 200
Kustaanheimo, P. E., & Stiefel, E. L. 1965, J. Reine Angew. Math., 208, 204
Lousto, C., & Zlochower, Y. 2008, PhRvD, 77, 044028
Lousto, C. O., Campanelli, M., Zlochower, Y., & Nakano, H. 2010, CQGra, 27, 114006
Lousto, C. O., Nakano, H., Zlochower, Y., & Campanelli, M. 2010, PhRvL, 81, 084023
Lousto, C. O., & Zlochower, Y. 2011a, PhRvL, 107, 231102
Lousto, C. O., & Zlochower, Y. 2011b, PhRvD, 83, 024003
Makino, J., & Aarseth, S. J. 1992, PASJ, 44, 141
Makino, J., Fukushige, T., Koga, M., & Namura, K. 2003, PASJ, 55, 1163
Merritt, D., Schnittman, J. D., & Komossa, S. 2009, ApJ, 699, 1690
Pellerin, A., Meurer, G. R., Bekki, K., et al. 2010, AJ, 139, 1369
Peterson, C. J., & King, I. R. 1975, AJ, 80, 427
Plummer, H. C. 1911, MNRAS, 71, 460
Portegies Zwart, S. F., Baumgardt, H., Hut, P., Makino, J., & McMillan, S. L. W. 2004, Natur, 428, 724
Portegies Zwart, S. F., & McMillan, S. L. W. 2000, ApJL, 528, L17
Pretorius, F. 2005, PhRvL, 95, 121101
Sopuerta, C. F., Yunes, N., & Laguna, P. 2006, PhRvD, 74, 124010
Suzuki, T. K., Nakasato, N., Baumgardt, H., et al. 2007, ApJ, 668, 435
Toomre, A. 1977, in The Evolution of Galaxies and Stellar Populations, ed. B. M. Tinsley & R. B. Larson (New Haven, CT: Yale University Observatory)
van Meter, J. R., Miller, M. C., Baker, J. G., Boggs, W. D., & Kelly, B. J. 2010, ApJ, 719, 1427
Whitmore, B. 2006, Massive Stars: From Pop III and GRBs to the Milky Way (Cambridge: Cambridge Univ. Press)
Whitmore, B., Zhang, Q., Leitherer, C., & Fall, M. 1999, AJ, 118, 1551
Whitmore, B. C., Chandar, R., Schweizer, F., et al. 2010, AJ, 140, 75
Zhang, Q., & Fall, S. M. 1999, ApJL, 527, L81
Zlochower, Y., Campanelli, M., & Lousto, C. O. 2010, CQGra, 28, 114015